Advances in Biochemistry and Biotechnology
Shibafuji Y, et al. Adv Biochem Biotechnol 8: 10113.
www.doi.org/10.29011/2574-7258.010113
www.gavinpublishers.com

Research Article

Antibody Productivity of CHO Cells is Altered by ER Stress Tolerance of the Host Cell

Shibafuji Y[1], Nagao N[1], Nagashima Y[2], Kawano Y[1], Ishino T[1,3], Yohda M[2*], Kurata H[1,2]

[1]Yokohama Technical Center, AGC Inc., Yokohama,Kanagawa, Japan.

[2]Department of Biotechnology and Life Science, Tokyo University of Agriculture and Technology, Tokyo, Japan.

[3]AGC Biologics, Washington, USA.

[*]**Corresponding author:** Masafumi Yohda, 2-24-16, Naka-cho, Koganei-shi, Tokyo 184-8588 Japan.

Citation: Shibafuji Y, Nagao N, Nagashima Y, Kawano Y, Ishino T, et al. (2024) Antibody Productivity of CHO Cells is Altered by ER Stress Tolerance of the Host Cell. Adv Biochem Biotechnol 8: 10113. DOI: https://doi.org/10.29011/2574-7258.010113

Received Date: 29 February, 2024; **Accepted Date:** 05 March, 2024; **Published Date:** 08 March, 2024

Abstract

We compared high- and low-producing Chinese hamster ovary (CHO) cell clones of two types of antibodies to explore the factors involved in the antibody productivity. A comparison of antibody gene copy numbers showed that, as expected, more genes were introduced in the genomes of the high-producing clones than in the genomes of the low-producing clones. However, specific productivity (Qp) was not in a direct proportional relationship to gene copy numbers and the quantities of mRNAs. The Qp values were lower than the values expected by the increase of genes or mRNAs, which may have been due to the limited rates of transcription and translation. Further comparisons were performed by proteome analyses. The results showed that endoplasmic reticulum (ER) stress occurred in the low-producing clones, resulting in apoptosis. The expression of genes related to the TCA cycle was decreased in cells with low viable cell density (VCD), even in high-producing clones. These results indicate that CHO host cells are diverse, with some cells tolerant to ER stress and others less tolerant. For less tolerant cells, ER stress is induced by antibody production, and their viability is reduced by apoptosis. Consequently, only clones with low copy numbers and low production were produced. On the other hand, the ER stress-tolerant cells yielded high-producing clones with high copy numbers. However, VCD is thought to decrease as Qp increases. These results indicate that suppression of ER stress associated with high antibody production is important for antibody production by CHO cells.

Keywords: CHO; Antibody; Proteomics; Titer; Gene copy number; ER stress;

Abbreviations:

CHO - Chinese hamster ovary; Qp - Specific productivity; ER - Endoplasmic reticulum; IgG - Immunoglobulin G; HC – Heavy chain; LC - Light chain; LC-MS - Liquid chromatography-mass spectrometry; mAb - Monoclonal antibody; VCD - Viable cell density; Via – Viability

Introduction

Biopharmaceuticals are pharmaceutical drug products manufactured by biotechnology. Among biopharmaceuticals, antibody drugs have attracted considerable attention recently owing to their high specificity for their targets and fewer side effects. In the 2000s, they became the top sellers among new drugs in the pharmaceutical industry [1, 2]. Due to their complex structure, antibody drugs, which include numerous disulfide bonds and glycosylation, are produced using animal cells. Among various mammalian cells, the most frequently used cell today is the Chinese hamster ovary (CHO) cell. CHO cells have been used for the production of biopharmaceuticals other than antibodies such as tissue plasminogen activator [3] or erythropoietin [4]. They are also recognized as the most compatible with antibody drugs from the viewpoints of high productivity, quality of glycan structures, and safety [5]. Therefore, most antibody drugs use CHO cells as host cells in their production systems [1, 2, 6]. However, the expression yield by CHO cells was initially less than 50 mg/L culture. Since

the medication dosage for antibody drugs is significantly larger than that of conventional biopharmaceuticals, the increase in productivity was indispensable for the development of these drugs. Due to technological breakthroughs in cell processing and culture media, the productivity of CHO cells for antibody production has increased to 5 g/L, and in some cases, even more than 10 g/L [7-9]. Generally, antibody-drug production cell lines are constructed using CHO cells as host cells by transfection with the target genes. The plasmid containing the target gene is randomly inserted into the chromosome of the host cell, resulting in a large variation in protein expression among the production clones. The selection of clones stably expressing large amounts of antibodies is a time-consuming and labor-intensive process. Many possible factors determine the production yield. It is affected by the copy number of the gene inserted into the chromosome, the process of transcription to mRNA, the process of translation to polypeptides, protein modification, folding, and even secretion outside the cell, as well as the efficiency of each step [10]. It is not well understood which characteristics determine the expression yield. In this study, we aimed to understand the differences between high- and low-producing clones.

The expression level of the target genes in mammalian cells is mainly affected by the state of the chromosome region integrated by the gene of interest, the copy number of the target gene, and its transcription and translation efficiency [11]. We compared high- and low-producing clones of two types of antibodies to explore the factors involved in the antibody productivity of CHO cells. The high-producing clones had almost the same titer, but the viable cell densities (VCDs) were very different. This result suggests that a larger specific productivity (Qp) affects proliferation. Interestingly, the low-producing clones with low Qp had a smaller VCD, indicating a decrease in viability at an earlier stage. A comparison of antibody gene copy numbers showed that, as expected, more genes were introduced in the high-producing clones than in the low-producing clones. However, Qp was not in a direct proportional relationship to gene copy numbers and the quantities of mRNAs. Qp values were less than the values expected by the increase in gene copy numbers or the amounts of mRNAs, which may be due to the limited rates of transcription and translation. Further comparisons were made by proteome analyses. The results showed that ER stress occurred in the low-producing clones, suggesting that ER stress-induced apoptosis reduced viability. The expression of genes related to the TCA cycle was decreased in cells with low VCD, even in high-producing clones. These results indicate that CHO host cells are diverse, with some cells tolerant to ER stress and others less tolerant. For less tolerant cells, ER stress was induced by antibody production, and their viability was reduced by apoptosis. Therefore, it can be surmised that only clones with low copy numbers and low production were produced. On the other hand, the cells with high ER stress tolerance yielded high-producing clones with high copy numbers. However, VCD is thought to decrease as Qp increases. These results indicate that suppression of ER stress associated with high antibody production is important for antibody production by CHO cells.

Materials and Methods

Cell line and Cultivation

The clones used in this experiment were as follows: Two different human IgG1 GOI vectors were transfected into CHO DG44 cells [12], which were adapted to serum-free suspension cultures. After cloning, a total of 12 clones, three with relatively high productivity and three with relatively low productivity expressing the respective IgG1, were selected for further experiments.

Cell thawing and passaging: Basic medium heated to 37.0 °C in a water bath was added to 125-mL Erlenmeyer flasks, and the medium was conditioned in a shaker incubator. Cryopreserved vials containing cells were thawed in a hot water bath, placed in sterile centrifuge tubes containing basic medium, and centrifuged (220 × g, 5 min, rt). The supernatant was discarded, and the cell pellet was suspended in a flask containing basic medium to initiate cell culture. The incubation conditions were 37.0 °C, 125 rpm (25 mm orbital shake diameter), and 5% CO_2. Three days after the start of culture, VCD and viability were measured by the trypan blue exclusion method using a Vi-Cell BLU (Beckman Coulter); for Day 3 passages, the initial cell density was 3.0×10^5 cells/mL; for Day 2 passages, the initial cell density was 6.0×10^5 cells/mL for Day 2 passages, and the cell density was adjusted with fresh medium to achieve an initial cell density of 6.0×10^5 cells/mL for Day 3 passages.

The CHO fed-batch culture was performed as follows: Fed-batch cultures of CHO cells were subjected to shaker incubators using 125-mL Erlenmeyer flasks. Cultures were performed at 37.0 °C, 125 rpm (25 mm orbital shake diameter), 5% CO_2, using a proprietary chemically defined basal medium with a starting volume of 30 mL. The culture was performed three times for each clone (three biological replicates). The viable cell density at the start was inoculated at 0.5×10^6 cells/mL. A proprietary chemically defined feed medium consisting of amino acids, vitamins, trace elements, and glucose was used as the feed medium. The feed medium was added to the cell culture at Days 3, 6, 9 and 12. The cells were harvested on Day 14. Culture media with three biological replicates for each culture condition were sampled for viable cell density (VCD), viability, titer, metabolites, pH and osmolarity measurements at Days 3, 6, 9, 12 and 14. VCD and viability were measured by the trypan blue exclusion method using a Vi-CELL XR Cell Viability Analyzer (Beckman Coulter).Metabolites, glutamine, glutamic acid, glucose, lactic acid and ammonia, were measured using a Cedex Bio HT Analyzer (Roche). Osmolarity and pH were measured by a pH meter (S2K333, Toyorika, Tokyo, Japan) and osmolarity meter (OM-6060, Arkray, Kyoto, Japan).

Specific productivity (*Qp*) was calculated in pg/cell/day using the following equation where *DP* is the change in antibody titer between the first and last day of evaluation (μg/ml), n_0 and n_t are the live cell density at the start and end points (10^6 cells/ml), and *t* is the incubation time in days [13].

$$Qp = \frac{10ln\left(\frac{n_t}{n_o}\right)\Delta P}{(n_t - n_o)t}$$

Droplet Digital PCR

The number of antibody genes inserted into the CHO genome was determined by droplet digital PCR (Bio-Rad, Hercules, CA). Antibody-producing CHO cells (2×10^6 cells) in the exponential growth phase were collected by centrifugation (300 × g, 5 min, 2 °C). Genomic DNA was extracted by using the DNeasy Blood & Tissue Kit (QIAGEN, Venlo, Netherlands). Prior to PCR, the acquired genomic DNA was digested and fragmented with the restriction enzyme BspH I. The PCR was performed under the following thermal cycle conditions: hot start at 95 °C (10 min), followed by 50 cycles of [94 °C (30 sec), 59 °C (90 sec)], with enzyme deactivation at 98 °C (10 min).

The percentage of droplets in which PCR amplification took place was analyzed in the resulting Droplet Reader, and the number of inserted copies per cell was calculated relative to the value of the reference (Chinese hamster ß-microglobulin gene) [14]. The primers and probes are designed for the vector sequences of both ends of inserted IgG genes (Supplementary Table S1).

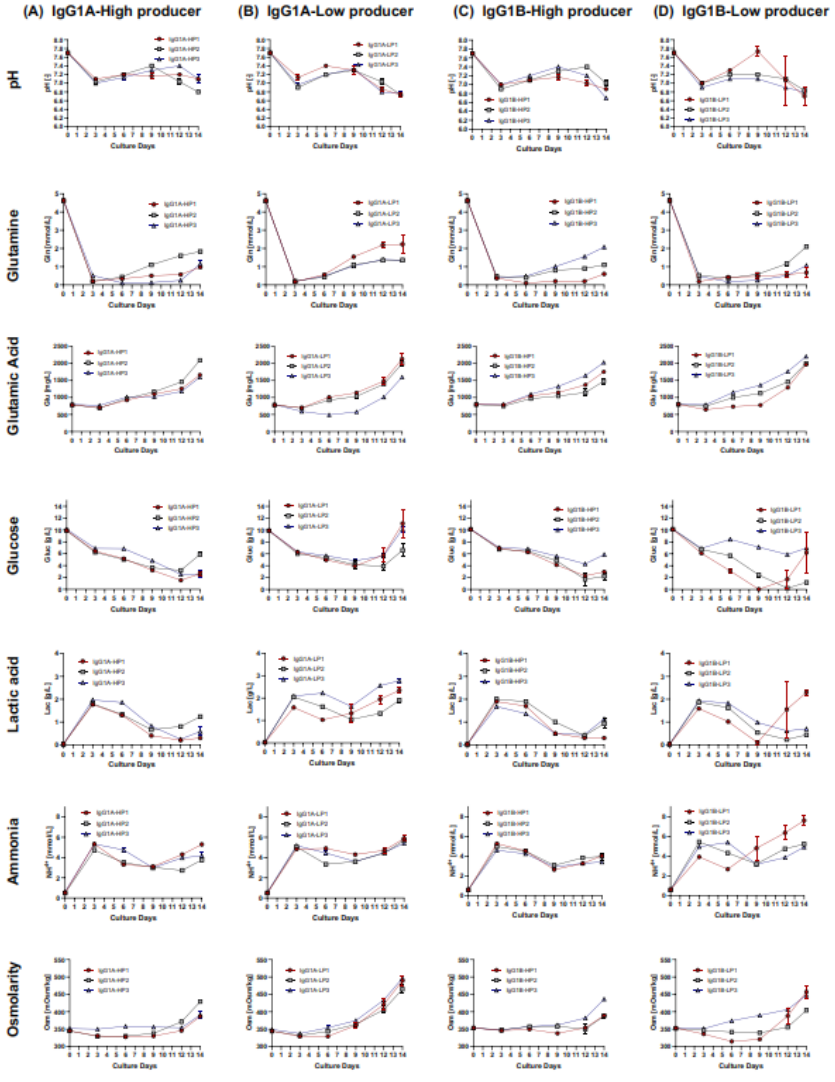

Figure S1: Culture trends of high and low producers. Each value represents the mean value (N = 3), and error bars represent the standard deviation. For each clone, the data for pH, glutamine, glutamic acid, glucose, lactic acid, ammonia, osmolarity and specific productivity are shown as graphs. (A) Culture data of clones with high IgG1A productivity. (B) Culture data of clones with low IgG1A productivity. (C) Culture data of clones with high IgG1B productivity. (D) Culture data of clones with low IgG1B productivity.

Quantitative real-time PCR

The mRNA expression levels of antibodies against heavy chain (HC) and light chain (LC) in CHO cells were determined by quantitative real-time PCR. Antibody-producing CHO cells (4×10^6 cells) in the middle stage of exponential growth in maintenance culture were collected by centrifugation (300 × g, 5 min, 2 °C). Total RNA was then produced by NucleoSpin RNA (TaKaRa Bio, Shiga, Japan). The acquired total RNA was analyzed for concentration and quality using Nanodrop and TapeStation, and cDNA was synthesized by the iScript™ Advanced cDNA Synthesis Kit for RT-qPCR (Bio-Rad). For quantitative real-time PCR, THUNDERBIRD SYBR qPCR Mix (TOYOBO, Osaka, Japan), the reaction solution was prepared to a final concentration of 0.1 µM of each primer, and PCRs were performed under the following thermal cycle conditions: hot start at 95 °C (1 min), followed by 50 cycles of [95 °C (15 sec), 60 °C (30 sec)].

The mRNA expression levels of HC and LC for each antibody were calculated relative to the value for the reference (Chinese hamster cyclophilin). The primer sequences are shown in Supplementary Table S1.

Proteomic Analysis

Sample preparation: Sampling was performed from the Day 6 fed-batch culture medium, and the supernatant was removed by centrifugation (14000 × g, 30 sec, 2 °C). For washing of the cell pellet, the cells were washed with 2 mL of ice-cold phosphate buffered saline (PBS) and centrifuged again (14000 × g, 30 sec, 2 °C) to remove the PBS. The resulting cell pellets were immediately stored at -80 °C.

The protein extraction and digestion were performed according to the method detailed in our previous manuscript [15] with a slight modification. Cell pellets were added to 2% SDS - 100 mM Tris-HCl (pH 8.5). Then, the cells were disrupted by sonication using a Bioruptor (CosmoBio, Tokyo, Japan), and the protein concentration was measured by BCA assay. Twenty micrograms of protein were aliquoted, and tris (2-carboxyethyl) phosphine hydrochloride (TCEP) was added to a final concentration of 23.8 mM and incubated at 80 °C for 10 min. Subsequently, iodoacetamide (IAA) was added at a final concentration of 31.3 mM and alkylated by incubation in the dark at room temperature for 30 min. To this reaction solution, 20 µL of 13.3 µg-solid/µL Sera-mag SpeedBead Carboxylate-Modified Magnetic Particles (1:1 mixture of hydrophilic and hydrophobic, Cytiva, Marlborough, MA) was added and mixed. Next, 99.5% ethanol was added at a final concentration of 71% and mixed for 10 min. The magnetic beads were separated on a magnetic stand, and the supernatant was discarded, washed with 80% ethanol, and further washed with acetonitrile. Air-dried beads were suspended in 100 µL 50 mM Tris-HCl (pH 8) and sonicated for 5 min. Quenching was performed by adding 20 µL of 5% TFA and mixing, and the magnetic beads were separated using a magnet stand. The supernatant was collected, desalted using GL-Tip SDB (GL sciences, Tokyo, Japan), centrifuged, concentrated using SpeedVac (Thermo Fisher Scientific), and resuspended in 2% acetonitrile - 0.1% TFA. The concentration of the produced peptide was determined by measuring the absorbance.

The LC-MS analysis was conducted as follows: Measurements were performed using a Thermo Scientific EASY-nLC1200 (Thermo Fisher Scientific) and Orbitrap Eclipse Tribrid mass spectrometer (Thermo Fisher Scientific). We used 0.1% formic acid as mobile phase A and 0.1% formic acid - 80% acetonitrile as mobile phase B. Acclaim PepMap 100 C18 (75 µm×12 cm, 3 µm, Thermo Fisher Scientific) was used as a trap column. A 500-ng peptide sample was injected into a NANO HPLC CAPILLARY COLUMN (75 µm × 12 cm, Nikkyo Technos, Tokyo, Japan) and separated at a column temperature of 35 °C and a flow rate of 200 nL/min. The gradient conditions were as follows: 6% B for 1 min, linear gradient to B 47% for 90 min, linear gradient to B 75% for 5 min, linear gradient to B 90% for 4 min, followed by 90% B for 15 min. Mass spectra were acquired in positive mode at a spray voltage of 2.0 kV. The MS1 scan range of m/z was 495–745, the resolution was 15,000, and the [DELETE]AGC [DELETE]target was 4×10^5. MS2 spectra were produced with a precursor range of m/z 500-740 or 502-738, a scan range of m/z 200-1800, resolution 60,000, the target 1.6×10^6, and DIA mode with an isolation window width of 4 Da.

Data analysis was conducted as follow: Data acquired by LC-MS were analyzed using DIA-NN version 1.8.1 [16]. First, the raw files were converted to mzML files using MSconvert version 3.0.20293 [17] and then to dia files using DIA-NN. Spectral libraries were created using Scaffold DIA and Prosit [18] based on the amino acid sequences (Cricetulus griseus CHOK1GS, Ensembl release 104) produced from Ensembl. DIA-NN parameters were set to a charge range of 2–4, peptide length range of 7–45, precursor ion m/z range of 495–745, and fragment ion m/z range. A second analysis was performed using the spectral library produced from the first analysis, and the quantitative values produced were used for downstream analysis. R version 4.3.0 [19] was used for data visualization, and clusterProfiler version 4.8.1 (NN-5) was used for the GO enrichment analysis [20].

Results

The workflow of this study is shown in Figure 1. DG-44 host cell lines were transfected with vectors containing the genes for the heavy chain (HC) and the light chain (LC) of two different monoclonal antibodies (mAbs) (IgG1A and IgG1B). Single-cell cloning was performed from the stably transfected cell pools. After confirmation of clonality, 48 randomly selected clones were cultured in 6-well plates, and antibody concentrations were measured when VCD decreased below 50%. The clones selected

for productivity and proliferation were sequentially scaled up from plate scale to shaker flask scale, and cells from each clone were stored. The three clones with the highest productivity (approximately 2 g/L) and the three clones with the lowest productivity (approximately 0.5 g/L) for IgG1A and IgG1B were selected. The 12 selected clones were applied for fed-batch cultures.

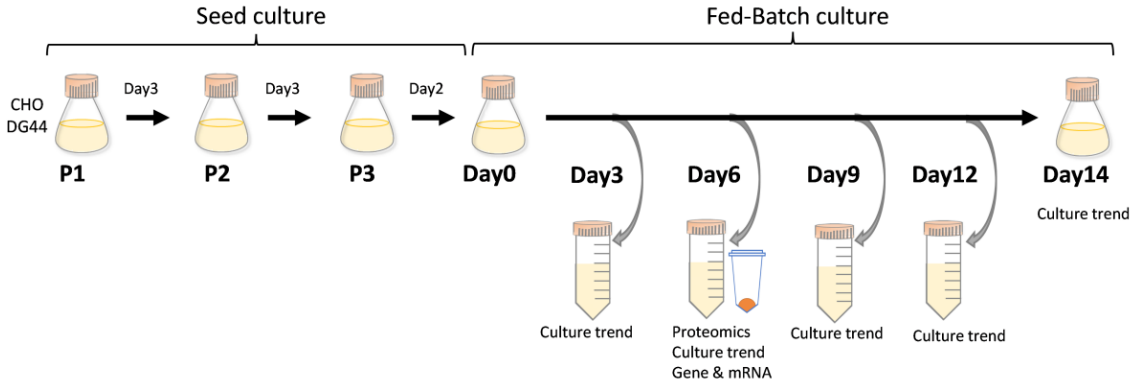

Figure 1: Schematic overview of seed and fed-batch culture. Bioprocess monitoring for fed-batch culture was carried out on Day0, Day3, Day6, Day9, Day12 and Day14 to assess viable cell density, viability, metabolite and titer. Samples on Day6 were prepared for copy number analysis, mRNA level analysis and proteomic profiling.

The fed-batch cultures were conducted in triplicate (N=3) for each of the selected clones and sampled at the intervals indicated in Figure 1 for culture trend analysis, proteome measurement, and quantification of copy number and mRNA content. Figure 2 illustrates the titer, VCD, viability, and Qp of high- and low-producing clones. Among the three high-producing clones of IgG1A, the titer was consistent, yet the VCD showed significant variance. Consequently, clones exhibiting higher Qp demonstrated lower VCD, indicating an inverse relationship between cell proliferation and antibody production. Conversely, all three IgG1A low-producing clones displayed low VCD, with a noticeable decline in viability from the initial stages of the culture, implying early-stage apoptosis. The metabolic profiles remained largely similar, except for differences in osmolarity and lactic acid levels (Supplementary Fig. S1). While high-producing clones exhibited lactic acid consumption, there was a minimal decrease in lactic acid in low-producing clones. Additionally, an increase in osmolarity was noted starting from the 6th day in low-producing cultures.

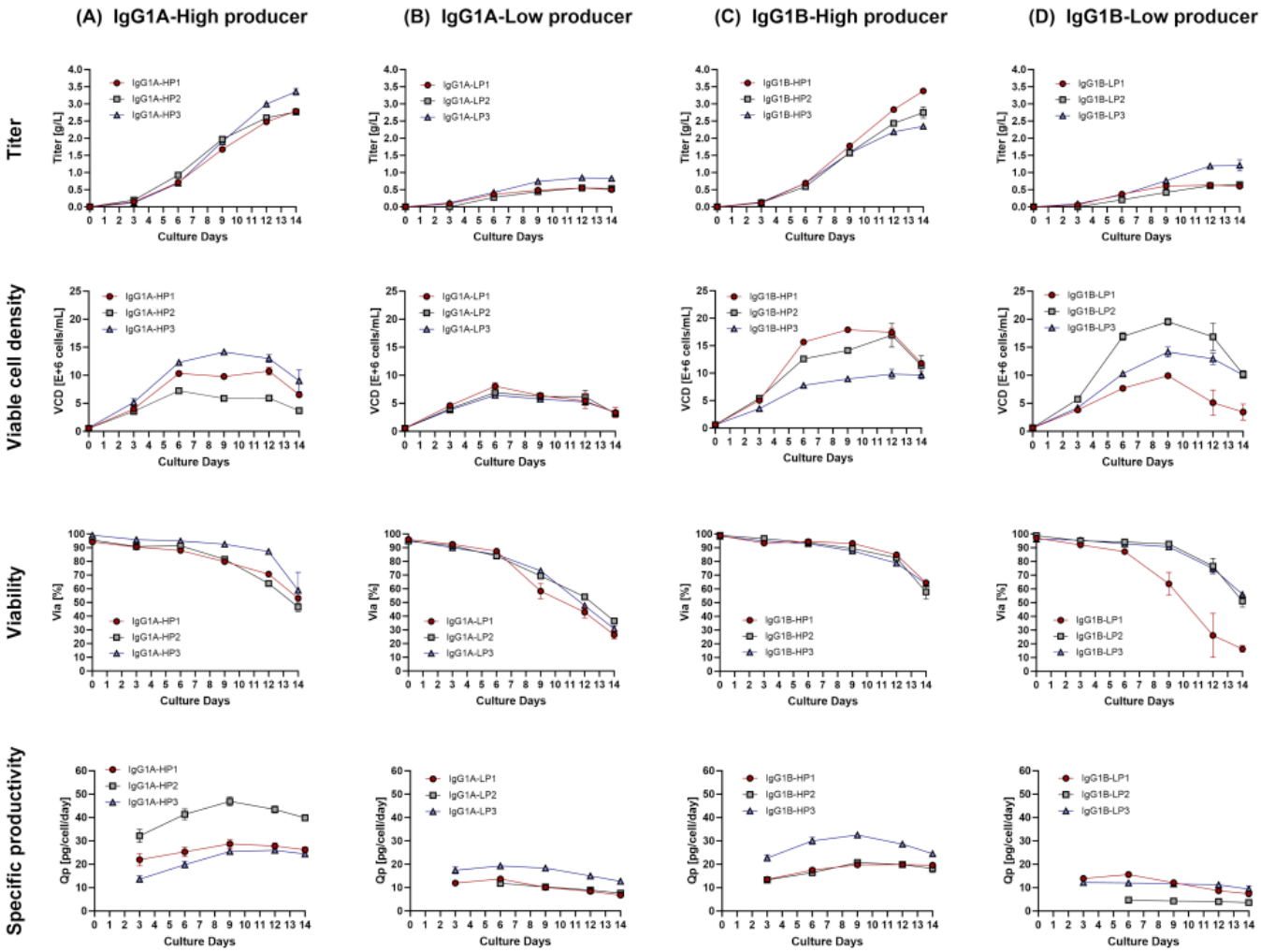

Figure 2: Culture trends of high and low producers. Each value represents the mean value (N = 3), and error bars represent the standard deviation. For each clone, the data for titer, viable cell density, viability and specific productivity are shown as graphs. (A) Culture data of clones with high IgG1A productivity. (B) Culture data of clones with low IgG1A productivity. (C) Culture data of clones with high IgG1B productivity. (D) Culture data of clones with low IgG1B productivity.

The high-producing IgG1B clones also show the same trend as the high-producing IgG1A clones, with larger Qp leading to lower VCD. The low-producing clone also differed greatly in VCD, as did the high-producing clone. Among them, an abrupt decrease in viability was observed for clone IgG1B-LP1, suggesting that apoptosis occurred in the early phase, similar to low-producing clones for IgG1A. IgG1B-LP1 showed a marked increase in lactic acid in the late incubation period, corresponding to a decrease in viability. The viability of the other two clones was similar to that of the high-producing clone.

Considering that the differences in titer and Qp should be due to differences in the copy number of the genes, the IgG gene copy number and the amount of IgG mRNA were measured (Fig. 3). The copy number was quantified at both ends of the transgene by digital PCR. Since both values were almost the same, it was determined that the full length of the gene was inserted. mRNA levels were measured by quantitative PCR for the transcript levels of HC and LC. As expected, the copy number of the gene in the low-producing clone was small. However, Qp was not in a direct proportional relationship to gene copy numbers and the quantities of mRNAs. Qp values were less than the values expected by the increase in gene copy numbers or the amounts of mRNAs, which may be due to the limited rates of transcription and translation. These results suggest that there are limits to the rates of transcription and translation. There is also a possibility of a gene location issue.

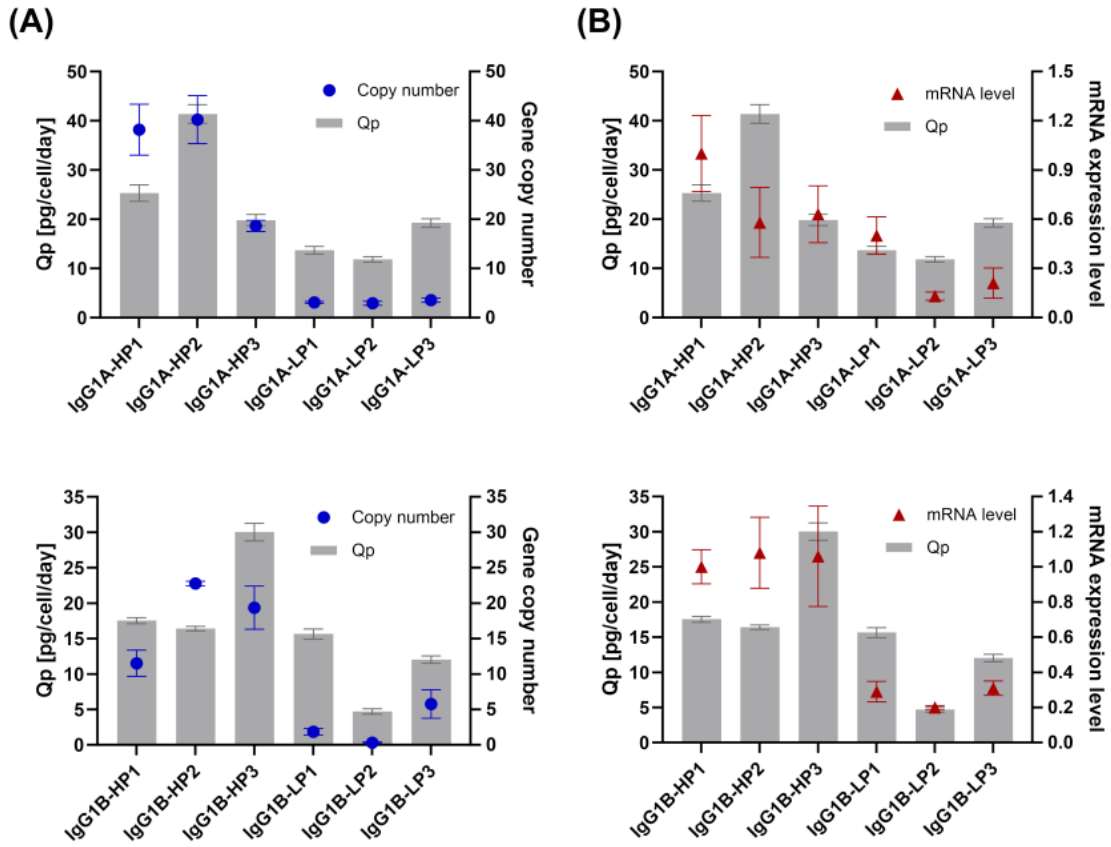

Figure 3: Comparative data on specific productivity (Qp) and gene copy number and mRNA of high and low producers. Each value represents the mean value (N = 3), and error bars represent the standard deviation. (A) Specific productivity (Qp) and gene copy number. (B) Specific productivity (Qp) and mRNA expression level.

The difference in titer is largely due to VCD and viability as well as Qp. To determine the cause of the difference in VCD and viability, proteome analyses were conducted. Since apoptosis seems to occur after Day 6 in IgG1A low-producing cells, sampling was performed on Day 6 for proteome analysis. Figure 4A shows the intracellular activities of the proteins that exhibited different behaviors between the high- and low-producing clones in the proteome analysis.

Among proteins related to protein hydration, prolyl 3-hydroxylase family member 4 (P3h4) may be associated with ER-phagy. P3h4 belongs to the Leprecan (leucine proline-enriched proteoglycans) family localized in the ER [21, 22] and forms a complex with prolyl 3-hydroxylase to regulate lysine hydroxylation in collagen [23]. It is known to be involved in selective ER-phagy [24]. These results suggest that ER-phagy may be induced in low-producing clones.

In the glycoprotein metabolic process, ERp44, an ER protein, was significantly induced in the low-producing clones. ERp44 is a molecular chaperone with a thioredoxin-like domain and has been reported to regulate oligomer formation in immunoglobulins and adiponectin, as well as the localization of redox enzymes Ero1 and Prdx4 in the endoplasmic reticulum [25]. This result suggests that some problems occurred in low-producing cells during the process of antibody formation in the endoplasmic reticulum.

In addition to ERp44, Prdx4 and Pdia5 were induced among the factors classified as protein folding. Prdx4 is an antioxidant enzyme belonging to the peroxiredoxin family. It reduces hydrogen peroxide and alkyl hydroperoxides using the reducing power of glutathione and other reducing agents. It may be used to remove peroxides associated with the formation of S-S bonds in antibody formation. On the other hand, Pdia5 contributes to the rearrangement of disulfide bonds in ATF6a under stress conditions, thereby promoting ATF6a efflux from the ER and activating target genes [26].

Among the factors involved in the endoplasmic reticulum, ERp44, TXNDC12, Edem3 and Erlec1 were highly expressed in low-producing clones. TXNDC12 (thioredoxin domain-containing protein 12) belongs to the thioredoxin superfamily, has a CXXC motif in its active center and is involved in redox regulation, protection against oxidative stress, and refolding of disulfide bond-containing proteins [27]. EDEM3 has alpha1,2-mannosidase activity and is involved in the pruning of mannose added to proteins in the endoplasmic reticulum and is said to be involved in ER-associated degradation of conformationally aberrant glycoproteins [28]. Erlec1 is a member of the ER-associated degradation surveillance system lectin and is involved in the degradation of misfolded glycoproteins in the ER [29].

Curiously, the increase in the representative ER stress marker Hspa5 was not observed in low-producing clones except IgG1B-LP3. In contrast, a slight increase in Hspa5 occurred in some high-producing clones. Typical ER stress markers, such as Hspa5, Ern1 (IRE1a), and ATF6, were not particularly altered in ER stress-related factors [30] (Fig. 4C). Among the three ER stress sensors (Ern1 (IRE1a), ATF6, Eif2ak3 (PERK)), the expression of Eif2ak3 (PERK) was induced in low-producing clones. The active form of PERK specifically phosphorylates its substrate eIF2a to repress cap-dependent translation. In this condition, the rate of translation throughout the cell is reduced, and the synthesis of new proteins inserted into the endoplasmic reticulum is decreased [30]. On the other hand, phosphorylated eIF2a induces the transcription factor ATF4. This PERK-ATF4 pathway also induces the expression of CHOP and GADD153, transcription factors involved in promoting apoptosis, thereby inducing apoptotic signals depending on the intensity or duration of ER stress.

In low-producing clones, oxidative stress, probably associated with antibody production, results in a stress response in which the PERK pathway in particular is predominantly activated and suppresses proliferation and apoptosis [31]. In contrast, the IRE1a pathway was suppressed.

Some of the high-producing clones also had suppressed VCD. Poorly proliferating clones showed a common trend in TCA cycle-related enzymes, regardless of productivity (Fig. 4D). The more poorly proliferating clones increased levels of the related enzymes to activate the TCA cycle. On the other hand, clones with good proliferation moved toward compensating for sugar metabolism, such as through upregulation of Pck2, rather than toward the TCA cycle.

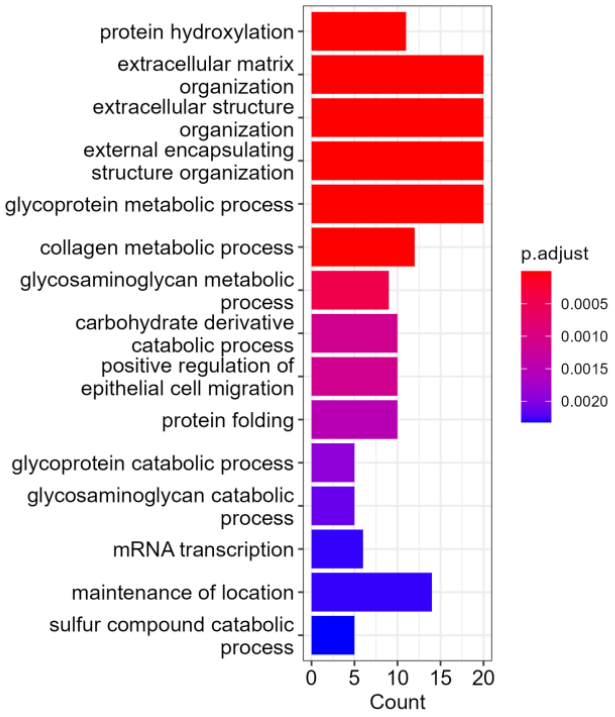

Figure 4A

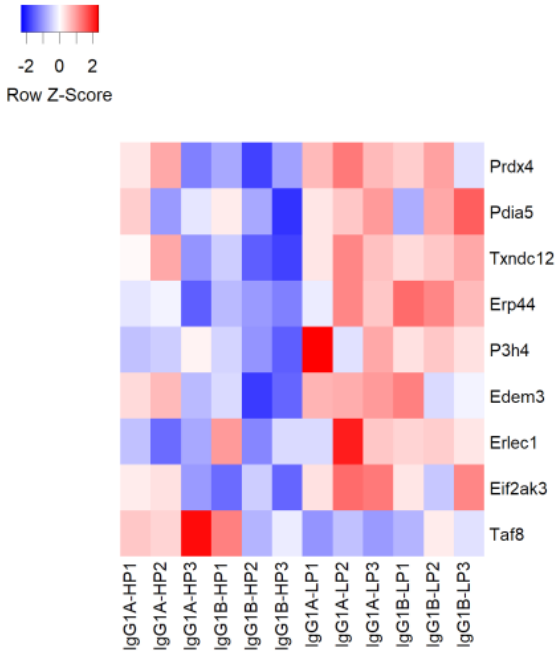

Figure 4B

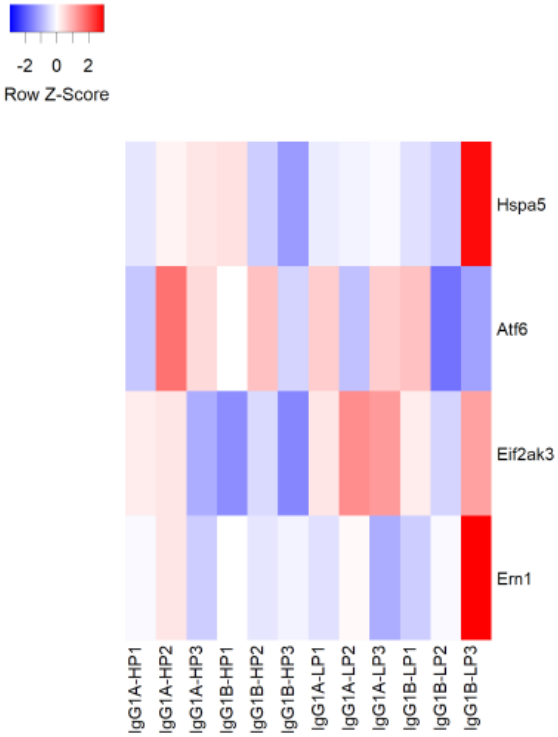

Figure 4C

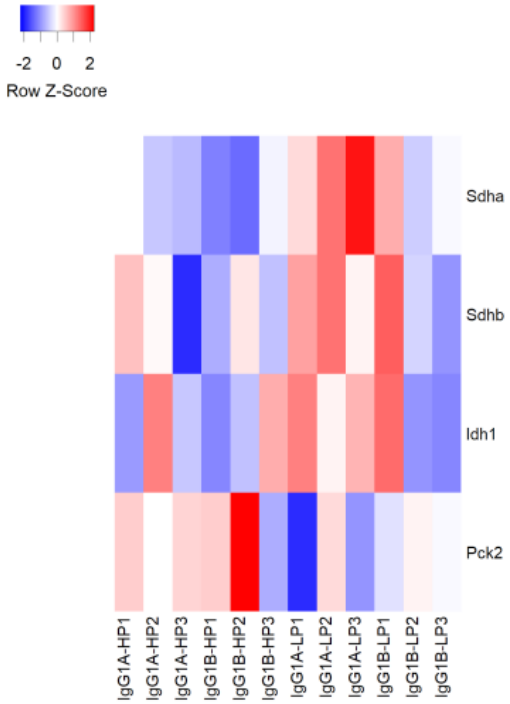

Figure 4D

Figure 4: Comparative analysis of protein expression between high- and low-producing clones. (A) Gene ontology (GO) enrichment analysis. Significantly enriched biological processes are shown. (B) Heatmap of ER stress, apoptosis, and transcription-related proteins. (C) Heatmap of ER stress marker and sensors (D) Heatmap of TCA cycle-related proteins and summary of the pathway.

Discussion

In this study, we compared high- and low-producing clones of two types of antibodies to explore the factors involved in the antibody productivity of CHO cells. Initially, we thought that the difference in productivity should reflect the copy number of genes. As expected, the gene copy numbers of high-producing clones were larger than those of low-producing clones. However, the Qp values in high-producing clones were less than the values evaluated from the copy numbers, which should be partly due to the limit of the rates for transcription and translation. In IgG1A high-producing clones, the high Qp strains showed relatively low VCD and viability. We thought that high IgG production would cause ER stress, resulting in low viability. However, in contrast, the VCD and viability of low producers were relatively low compared with high producers. Then, we compared them by proteome analyses.

While induction of the typical ER stress marker Hspa5 was not observed in low-producing clones except IgG1B-LP3, a slight increase occurred in some high-producing cells. However, other ER stress-related proteins were highly expressed in low-producing clones. Among ER stress sensors, the expression of PERK was high in low-producing cells. ATF6 expression was enhanced in almost all high-producing CHO clones, but the expression level of IRE1a was low. The characteristics of low producers are explained by the effect of activation of the PERK pathway. The PERK branch of the ER stress response is responsible for the transcriptional downregulation of platelet-derived growth receptor alpha and the attenuation of the IRE1a branch of the ER stress response [31].

It is challenging to attribute the difference between high- and low-producing clones solely to the expression of IgG. We think that the variation lies in the host cell lines; low-producing clones might originate from host cells relatively sensitive to ER stresses. The expression of IgGs in such ER stress-labile host cell clones could cause PERK-induced ER stresses, resulting in low VCD and viability. However, it remains unclear why the PERK branch is preferentially induced. PERK is known to regulate proinsulin trafficking and quality control in the secretory pathway [32]. The disulfide-rich IgG might specifically induce the PERK ER stress pathway, similar to insulin.

For less tolerant cells, ER stress is induced by antibody production, and their viability is reduced by apoptosis. Therefore, it can be surmised that only clones with low copy numbers and low production were produced. On the other hand, the cells with high ER stress tolerance yielded high-producing clones with high copy numbers.

There were differences between IgG1A- and IgG1B-producing cells, likely due to their distinct ER stress-prone propensity. As IgG1A low-producing cells are all affected by ER stresses, it seems that IgG1A is more problematic in folding and more likely to induce ER stress.

Antibodies have complex structures with numerous disulfide bonds. Their folding places a heavy burden on the ER. Thus, the ER stress response is an important issue in the mass production of antibodies in cells. The results of this study show that host cells are diverse and that their productivity differs due to the different ER stress responses associated with antibody production. In addition, antibody production is mainly activated by the PERK pathway, which induces decreased antibody production, growth inhibition and apoptosis. Furthermore, inhibition of the IRE1a pathway suppresses other ER stress pathways. High-producing clones were able to respond adequately to some degree to ER stress caused by antibody production but not to higher expression. It may be possible to construct clones with stable high expression by expression of endoplasmic reticulum chaperones involved in antibody structure formation and suppression of the PERK pathway.

Acknowledgements

We thank Toshimi Suzuki and Junichi Hasegawa for supporting all the cell culture works as well as Sayaka Ogino for LC-MS. We also appreciate that Kayla Been contributed for cell cloning.

Author Contributions

Conceptualization, Yusuke Shibafuji, Tetsuya Ishino, Masafumi Yohda and Hideyuki Kurata; methodology, Yusuke Shibafuji, Nobuyoshi Nagao and Yasuhiro Kawano; investigation, Yusuke Shibafuji, Nobuyoshi Nagao, Yuto Nagashima, and Yasuhiro Kawano; data curation, Yusuke Shibafuji, Nobuyoshi Nagao and Yasuhiro Kawano; writing—original draft preparation, Tetsuya Ishino, Masafumi Yohda, Hideyuki Kurata; writing—review and editing, Tetsuya Ishino, Masafumi Yohda and Hideyuki Kurata; visualization, Yusuke Shibafuji, Nobuyoshi Nagao and Yasuhiro Kawano; supervision, Tetsuya Ishino, Masafumi Yohda and Hideyuki Kurata; project administration, Masafumi Yohda and Hideyuki Kurata; funding acquisition, Hideyuki Kurata.

References

1. Walsh G (2018) Biopharmaceutical benchmarks 2018. Nat Biotechnol, 36: 1136-1145.
2. Kurata H, Ishino T, Ohshima Y, Yohda M (2022) CDMOs Play a Critical Role in the Biopharmaceutical Ecosystem. Front Bioeng Biotechnol 10: 841420.
3. Kaufman RJ, Wasley LC, Spiliotes AJ, Gossels SD, Latt SA, et al. (1985) Coamplification and coexpression of human tissue-type plasminogen activator and murine dihydrofolate reductase sequences in Chinese hamster ovary cells. Mol Cell Biol 5: 1750-1759.
4. Inoue N, Takeuchi M, Ohashi H, Suzuki T (1995) The production of recombinant human erythropoietin. Biotechnol Annu Rev 1: 297-313.
5. Kunert R, Reinhart D (2016) Advances in recombinant antibody manufacturing. Appl Microbiol Biotechnol, 100: 3451-3461.
6. Urquhart L (2020) Top companies and drugs by sales in 2019. Nat Rev Drug Discov 19: 228.
7. Handlogten MW, Lee-O'Brien A, Roy G, Levitskaya SV, Venkat R, et al. (2018) Intracellular response to process optimization and impact on productivity and product aggregates for a high-titer CHO cell process. Biotechnol Bioeng 115: 126-138.
8. Li F, Vijayasankaran N, Shen AY, Kiss R, Amanullah A (2010) Cell culture processes for monoclonal antibody production, MAbs 2: 466-479.
9. Weng Z, Jin J, Shao C, Li H (2020) Reduction of charge variants by CHO cell culture process optimization, Cytotechnology 72: 259-269.
10. Li ZM, Fan ZL, Wang XY, Wang TY (2022) Factors Affecting the Expression of Recombinant Protein and Improvement Strategies in Chinese Hamster Ovary Cells, Front Bioeng Biotechnol. 10: 880155.
11. Jiang Z, Huang Y, Sharfstein ST (2006) Regulation of recombinant monoclonal antibody production in chinese hamster ovary cells: a comparative study of gene copy number, mRNA level, and protein expression. Biotechnol Prog 22: 313-318.

12. Urlaub G, Mitchell PJ, Kas E, Chasin LA, Funanage VL, et al. (1986) Effect of gamma rays at the dihydrofolate reductase locus: deletions and inversions. Somat Cell Mol Genet 12: 555-566.

13. Ahmadi S, Davami F, Davoudi N, Nematpour F, Ahmadi M, et al. (2017) Monoclonal antibodies expression improvement in CHO cells by PiggyBac transposition regarding vectors ratios and design. PLoS One 12: e0179902.

14. Carver J, Ng D, Zhou M, Ko P, Zhan D, et al. (2020) Maximizing antibody production in a targeted integration host by optimization of subunit gene dosage and position. Biotechnol Prog 36: e2967.

15. Shibafuji Y, Nagao N, Yohda M (2023) Cystine and tyrosine feed reduces oxidative and ER stress in CHO cells. Biotechnol J 18: e2200638.

16. Demichev V, Messner CB, Vernardis SI, Lilley KS, Ralser M (2020) DIA-NN: neural networks and interference correction enable deep proteome coverage in high throughput. Nat Methods 17: 41-44.

17. Kessner D, Chambers M, Burke R, Agus D, Mallick P (2008) ProteoWizard: open source software for rapid proteomics tools development. Bioinformatics 24: 2534-2536.

18. Gessulat S, Schmidt T, Zolg DP, Samaras P, Schnatbaum K, et al. (2019) Prosit: proteome-wide prediction of peptide tandem mass spectra by deep learning. Nat Methods 16: 509-518.

19. Ihaka R, Gentleman R (1996) A language for data analysis and graphics. J. Comp. Graph. Stat. 5:299-314.

20. Wu T, Hu E, Xu S, Chen M, Guo P, et al. (2021) ClusterProfiler 4.0: A universal enrichment tool for interpreting omics data. Innovation (Camb) 2: 100141.

21. Ochs RL, Stein TW, Chan EK, Ruutu M, Tan E (1996) cDNA cloning and characterization of a novel nucleolar protein. Mol Biol Cell 7: 1015-1024.

22. Gruenwald K, Castagnola P, Besio R, Dimori M, Chen Y, et al. (2014) Sc65 is a novel endoplasmic reticulum protein that regulates bone mass homeostasis. J Bone Miner Res 29: 666-675.

23. Heard ME, Besio R, Weis M, Rai J, Hudson DM, et al. (2016) Sc65-Null Mice Provide Evidence for a Novel Endoplasmic Reticulum Complex Regulating Collagen Lysyl Hydroxylation. PLoS Genet 12: e1006002.

24. Ishii S, Chino H, Ode KL, Kurikawa Y, Ueda HR, et al. (2023) CCPG1 recognizes endoplasmic reticulum luminal proteins for selective ER-phagy. Mol Biol Cell 34: ar29.

25. Anelli T, Alessio M, Mezghrani A, Simmen T, Talamo F, et al. (2002) ERp44, a novel endoplasmic reticulum folding assistant of the thioredoxin family. EMBO J 21: 835-844.

26. Higa A, Taouji S, Lhomond S, Jensen D, Fernandez-Zapico ME, et al. (2014) Endoplasmic reticulum stress-activated transcription factor ATF6alpha requires the disulfide isomerase PDIA5 to modulate chemoresistance. Mol Cell Biol 34: 1839-1849.

27. Liu F, Rong YP, Zeng LC, Zhang X, Han ZG (2003) Isolation and characterization of a novel human thioredoxin-like gene hTLP19 encoding a secretory protein. Gene 315: 71-78.

28. Hirao K, Natsuka Y, Tamura T, Wada I, Morito D, et al. (2006) EDEM3, a soluble EDEM homolog, enhances glycoprotein endoplasmic reticulum-associated degradation and mannose trimming. J Biol Chem 281: 9650-9658.

29. Yoshida Y, Tanaka K (2010) Lectin-like ERAD players in ER and cytosol, Biochim Biophys Acta 1800: 172-180.

30. Gardner BM, Pincus D, Gotthardt K, Gallagher CM, et al. (2013) Endoplasmic reticulum stress sensing in the unfolded protein response. Cold Spring Harb Perspect Biol 5: a013169.

31. Castellano BM, Tang D, Marsters S, Lam C, Liu P, et al. (2023) Activation of the PERK branch of the unfolded protein response during production reduces specific productivity in CHO cells via downregulation of PDGFRa and IRE1a signaling. Biotechnol Prog 39: e3354.

32. Gupta S, McGrath B, Cavener DR (2010) PERK (EIF2AK3) regulates proinsulin trafficking and quality control in the secretory pathway. Diabetes 59: 1937-1947.